Extension of the hard-sphere particle-wall collision model to account for particle deposition

Pawel Kosinski and Alex C. Hoffmann

Department of Physics and Technology Bergen, The University of Bergen, N-5007 Bergen, Norway

(Received 14 March 2009; revised manuscript received 12 May 2009; published 10 June 2009)

Numerical simulations of flows of fluids with granular materials using the Eulerian-Lagrangian approach involve the problem of modeling of collisions: both between the particles and particles with walls. One of the most popular techniques is the hard-sphere model. This model, however, has a major drawback in that it does not take into account cohesive or adhesive forces. In this paper we develop an extension to a well-known hard-sphere model for modeling particle-wall interactions, making it possible to account for adhesion. The model is able to account for virtually any physical interaction, such as van der Waals forces or liquid bridging. In this paper we focus on the derivation of the new model and we show some computational results.

I. INTRODUCTION

One of the techniques used for simulating of two-phase flows is the Eulerian-Lagrangian approach, where the solid phase is modeled as a system of individual points, subject to forces according to their size and shape. The forces acting on the particles and causing them to move are a result of the interaction with the flow and collisions with other particles and containing walls. An important issue when investigating such flows using this approach is the proper modeling of these collisions.

There are various methods for this. The two main types of models are hard-sphere models and the soft-sphere models (see, for instance, Crowe *et al.* [1]). The difference between them is in how particle deformation and friction during impact are treated. In the hard-sphere model the concept of particle deformation and frictional sliding may be involved in the derivation of the model, but they do not appear in the mathematical formulation, which is in terms of impulse equations. In the soft-sphere model, on the other hand, "mechanical elements" such as a spring, dash pot, and friction slider are used to mimic the behavior of the two colliding particles or a particle colliding with a wall and their actions are described by differential equations.

In this paper we focus on the first type of model: the hard-sphere model. Hard-sphere models are used extensively in the numerical simulation of particle or fluid-particle systems. Particularly popular has been the simulation of fluidized beds (see, for example, references [2–5], this topic was recently reviewed by Deen *et al.* [6]) and two or three phase flows in pipes or reactors (e.g., references [7–13]). Moreover, it has been used for studying fast flows with particles, like shock waves interacting with dusts or explosions (see, for example, our previous works: [14–16]).

Two hard-sphere collision models are widely used, that of Hoomans *et al.* [17], and that of Crowe *et al.* [1]. Neither of these models takes into account cohesion between the particles or adhesion of a particle to a wall. As a result particles will always, unless the collision is made complete inelastic by setting the coefficient of restitution to zero, bounce off after a collision, even though their initial speed, size, and surface properties indicate that they should not escape the collision but adhere resulting in the formation of an agglomerate.

There are many processes in industry where this is of importance. Some examples are: the formation of hydrate or wax plugs in pipelines in the oil and gas industries, manufacturing of carbon black or fluidized beds processes where the particles are very fine or sticky.

Much of the work in the published research literature aimed at modeling particle cohesion has, until now, been dedicated to the simulation of fluidized beds. Reviews of the role played by interparticle cohesion in fluidized beds have been written by Visser [18] and Seville *et al.* [19].

Basically cohesive forces can be included in Eulerian-Lagrangian simulations in two ways. The first strategy is to include the cohesive force in the particle equation of motion and thus simply include it as an extra force acting on the particle in the numerical scheme. Most of the published literature has been focused on this approach using soft-sphere collision models. Some examples are: Mikami *et al.* [20], who extended the classical soft-sphere collision model of Tsuji *et al.* [21] with an extra nonlinear spring and a rupture joint to account for the cohesive force exerted between particles connected by a stretching liquid bridge, which ruptures at a given critical surface separation. In another context, Lian *et al.* [22] studied the collision of pendular-state agglomerates, building on their earlier work to characterize the cohesive forces arising from pendular bridges [23].

Also the behavior of dry granular materials that are so fine that surface forces play a role in their macroscopic behavior have been studied using this strategy. Baxter *et al.* [24] studied problems with the flow of granular materials arising from van der Waals forces, modeled by a Lennard-Jones type potential, including short-range repulsion, but modified to allow for some particle deformation, and the associated cohesion, in the contact point. Ye *et al.* studied the fluidization of fine powders (Geldart Group A) modeling particle cohesion with a Hamaker-type interaction, but without including short-range repulsion. To avoid the singularity at particle contact, the force was cutoff at a finite surface separation, chosen so that it is consistent with the physics of a contact point [25]. Pandit *et al.* [26] also studied the particulate fluidization of Geldart Group A powders using a Hamaker-type particle interaction.

The second strategy is what we are going to focus on in this paper. In this approach, the cohesive force is incorporated directly into an impulse-based collision model. We thus

aim to extend the hard-sphere model so that it becomes possible to account for cohesion or adhesion processes.

We note at this stage that in fluidized systems or granular flow, which most of the above references are concerned with, it may be convenient to incorporate the particle interaction force in the particle equation of motion, and thus directly in the numerical scheme. Complexity in the form of the interaction force law, $F(D)$, is then less of a problem. However, in more dilute flows, where the particle displacement within one time-step may be much higher, it is not computationally efficient to simulate the interaction directly in this way. Rather incorporating the interaction in the collision model would be more desirable. Another advantage of incorporating interparticle or particle-wall interaction in an impulse-based collision model is, as pointed out by Weber *et al.* [27] that such a collision model may be incorporated in continuum schemes for the simulation of the dynamics of a dispersed phase.

Perhaps the most relevant papers for the present paper are the two articles by Hrenya and co-workers [27,28]. In these papers they introduced a very simple particle interaction potential suitable for incorporation in a hard-sphere collision model, although they stopped short of formulating such a model themselves. Rather than using the full Hamaker interaction, allowed a dirac-delta-type attractive force to act between two particles at a certain surface separation, creating a square-well potential from which two colliding particles might or might not escape after a collision, depending on the velocity of impact and the coefficient of restitution. The reason for using this simple interaction law is that a law suitable for implementation in impulse-type particle collision models needs to be very simple.

Hard-sphere models, e.g., the one of Crowe *et al.* [1], which we will be working with here, are based on estimating the impulses (time-integrated forces) acting on particles during specified periods during the collision, due, for instance, to elastic/plastic deformation, and thus estimate translational velocity changes:

$$\Delta v = \int F dt, \tag{1}$$

with a similar time-integrated equation for the change in the rate of particle rotation incurred by an angular impulse (moment of impulse, see also below).

As Hrenya and co-workers point out that implementation in such a model of a given functional form for F as a function of surface separation, D, is not straight forward since the time-integral depends on the time that the particle spends within the F field, which depends not only on the approach and departure velocities to and from the collision but also, due to the particles' reaction to F, on F itself. This makes it impossible to find an analytical solution to Eq. (1) even for the simple form of the Hamaker interaction without the repulsion term. Hrenya and co-workers tackle this problem by tweaking the depth of their square-well potential so that it matches numerical simulations of Hamaker interactions.

It is not the focus of this paper to determine the best functional form for F. We mention two theories for interac-
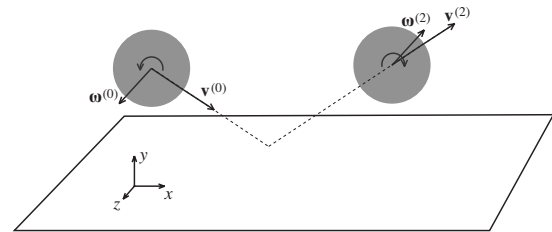

FIG. 1. Situation sketch.

tion that are more complete than Hamaker interaction between rigid bodies: the Johnson-Kendall-Roberts theory [29] criticized subsequently by Derjaguin *et al.* [30], leading to the formulation of the so-called Derjaguin-Muller-Toporov (DMT) theory. These theories are based on the analysis of the interaction between bodies deformed due to a normal load (e.g., as a consequence of a collision).

We recount those features of the hard-sphere model of Crowe *et al.* that will be relevant in the derivation of our extension to the model:

(i) The collision process is divided into two periods: *compression*, where the material of the particles is deformed and *recovery*, where the force due to elastic deformation is released.

(ii) The model takes into account the fact that the particle may slide along the surface upon which it impacts for some or all of the collision period. If it stops sliding it rolls over the surface for the rest of the collision period. The model distinguishes between three cases:

(I) the particle stops sliding during the compression period;

(II) the particle stops sliding during the recovery period, and

(III) the particle continues to slide throughout the entire collision.

(iii) The model is formulated in a Cartesian coordinate system where the y axis is normal to—and pointing away from—the wall on which the particle impacts (see Fig. 1).

The main application of this research is to model solid particles that are present in industry (e.g., in the transport of solids, in fluidized beds, catalyst particles, dusts in mines), including very small particles (e.g., aerosols, soot). We are, however, focusing not on applications but on physical aspects: the extension of an existing model to account for more complex physical interactions (adhesion).

In this paper, we are considering the point in time where a particle collides with a solid wall. The period of collision is so short that the impulses due to the normal fluid-dynamic forces acting on the particle, such as drag and lift, are negligibly small. The only fluid-dynamic force that is relevant to our model is that due to the fluid between the particle and the wall, which is squeezed out during the approach and sucked in during the departure [1]. We will discuss how to take this into account in Sec. II F.

II. DERIVATION

The standard hard-sphere model is quite extensively described in Crowe *et al.* [1] and therefore we base our exten-
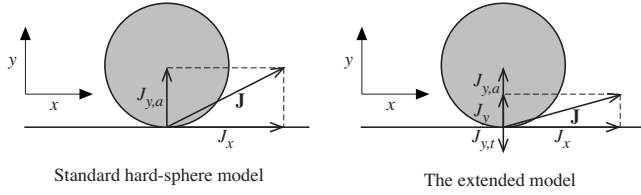
FIG. 2. A two-dimensional illustration of the difference between the standard hard-sphere model and the extended one.

sion on the formulation and notation from this reference. The interested reader may also find descriptions of the model in other sources, e.g., Refs. [31–33].

Following the notation of Crowe *et al.*, we denote the above-mentioned periods of the collision by superscripts. For the translational and angular particle velocities, **v** and **ω**, respectively, we denote by superscript (0), (1), (2), and (*s*) the values before the collision, at the end of the compression period, at the end of the recovery period and at the end of the sliding period, respectively. The notations for the impulses are different for the different cases and are given below.

A. Case I

1. Model—impulse equations

In this case, as mentioned, the particle stops sliding during the compression period. For the impulse components, $J_i = \int F_i dt$, we denote by superscript (1), (2), and (*s*) the impulses during the compression, the recovery and the sliding periods, respectively, and by superscript (*r*) the impulse during the "remainder" of the compression period after the particle has stopped sliding.

The set of impulse equations in the *y* direction in the model of Crowe *et al.* [1] for the sliding period is

$$m(v_x^{(s)} - v_x^{(0)}) = J_x^{(s)}, \tag{2a}$$

$$m(v_y^{(s)} - v_y^{(0)}) = J_y^{(s)}, \tag{2b}$$

$$m(v_z^{(s)} - v_z^{(0)}) = J_z^{(s)}. \tag{2c}$$

The impulse acting on the particle in the *y* direction $J_y^{(s)} = \int F_y dt$ is due to the deformation of the particle material: the compression and subsequent recovery during the collision. Part of the deformation will be elastic, and part plastic, the latter giving rise to a dissipative loss of mechanical energy, accounted for by a coefficient of restitution in the model of Crowe *et al.*

This force/impulse acting on the particle is always directed away from the wall on which the particle impacts, and is responsible for particle bouncing off the surface. The hard-sphere model does not consider any other forces acting along *y* axis.

In the extension to this model we will implement another force, acting toward the wall surface—allowing for phenomena like adhesion (see Fig. 2). We thus operate with an additional impulse $\mathbf{J}_t = (0, J_{y,t}, 0)$ so that the above model equation is modified to

$$m(v_x^{(s)} - v_x^{(0)}) = J_x^{(s)}, \tag{3a}$$

$$m(v_y^{(s)} - v_y^{(0)}) = J_{y,a}^{(s)} + J_{y,t}^{(s)}, \tag{3b}$$

$$m(v_z^{(s)} - v_z^{(0)}) = J_z^{(s)}. \tag{3c}$$

We have thus replaced the impulse component $J_y^{(s)}$ from Eq. (2b) by $J_{y,a}^{(s)} + J_{y,t}^{(s)}$. $J_{y,a}^{(s)}$ is the same as the impulse $J_y^{(s)}$ in Eq. (2b). The subscript y, a denotes that the impulse is directed away from the plane of impact, and it is therefore always positive in our coordinate system. This impulse is, as mentioned, due to the compression and recovery of the particle material.

The impulse $J_{y,t}^{(s)} = \int_s F_{y,t} dt$ is directed toward the plane of impact and is therefore always negative. It is caused by adhesive forces, whatever their origin. This completes our discussion of the first stage of the collision.

The same discussion applies to the two other stages of the collision. For the remainder of the compression period during which the particle has stopped sliding, we have the following equations:

$$m(v_x^{(1)} - v_x^{(s)}) = J_x^{(r)}, \tag{4a}$$

$$m(v_y^{(1)} - v_y^{(s)}) = J_{y,a}^{(r)} + J_{y,t}^{(r)}, \tag{4b}$$

$$m(v_z^{(1)} - v_z^{(s)}) = J_z^{(r)}. \tag{4c}$$

And for the last period (the recovery period)

$$m(v_x^{(2)} - v_x^{(1)}) = J_x^{(2)}, \tag{5a}$$

$$m(v_y^{(2)} - v_y^{(1)}) = J_{y,a}^{(2)} + J_{y,t}^{(2)}, \tag{5b}$$

$$m(v_z^{(2)} - v_z^{(1)}) = J_z^{(2)}. \tag{5c}$$

We note that the attractive force during a collision actually begins to act slightly before the surfaces touch and that they persist until the surfaces are removed some small distance from each other after the collision. Thus formally we include these small time intervals before and after contact during which the attractive force is active in the "compression" and "recovery" periods, respectively. This will not change the $J_{y,a}$ substantially, the time integrals of the elastic force remain the same.

A small change in $J_{y,a}$ will, however, be caused by the short-range attractive force accelerating the particle toward the surface on which it impacts, giving rise to an increase in $J_{y,a}$. Another effect, which in turn will lower $J_{y,a}$, and is not taken into account here or in the original model, is the deceleration of the impacting particle due to the outflow of fluid from the narrow gap between the on-coming particle and the surface on which it impacts [1]. Effects of this type can be included in later refinements of the model.

Finally we work out the model for the rotation, which, for this case, is the same as in the standard hard-sphere model, because it does not contain the impulse in the *y* direction,

$$I(\omega_x^{(s)} - \omega_x^{(0)}) = -aJ_z^{(s)}, \tag{6a}$$

$$I(\omega_y^{(s)} - \omega_y^{(0)}) = 0, \tag{6b}$$

$$I(\omega_z^{(s)} - \omega_z^{(0)}) = aJ_x^{(s)}, \tag{6c}$$

$$I(\omega_x^{(1)} - \omega_x^{(s)}) = -aJ_z^{(r)}, \tag{6d}$$

$$I(\omega_y^{(1)} - \omega_y^{(s)}) = 0, \tag{6e}$$

$$I(\omega_z^{(1)} - \omega_z^{(s)}) = aJ_x^{(r)}, \tag{6f}$$

$$I(\omega_x^{(2)} - \omega_x^{(1)}) = -aJ_z^{(2)}, \tag{6g}$$

$$I(\omega_y^{(2)} - \omega_y^{(1)}) = 0, \tag{6h}$$

$$I(\omega_z^{(2)} - \omega_z^{(1)}) = aJ_x^{(2)}. \tag{6i}$$

Here we make use of the fundamental equation from dynamics: $I(\Delta\omega) = \mathbf{r} \times \mathbf{J}$, where $\mathbf{r} = (0, -a, 0)$ and a is particle radius.

Physically, these equations evaluate the change in rotation of the particle due to the time integral of the moment, around the particle center of mass, of the force acting in the contact point during the sliding period.

We note that, even though the equations for this case may be the same as in the original model, a larger normal force acting in the contact point due to the force $F_{y,t}$ will cause a higher frictional moment to act on the particle, and may change a case II into a case I or a case III into a case II.

Finally we add three equations describing conditions on the surface velocity of the particle at the point of contact at particular instants during the collision. These are given in [1] but we repeat them here because they will be used below:

$$(v_x^{(s)} + a\omega_z^{(s)})\mathbf{i} + (v_z^{(s)} - a\omega_x^{(s)})\mathbf{k} = 0, \tag{7a}$$

$$(v_x^{(1)} + a\omega_z^{(1)})\mathbf{i} + v_y^{(1)}\mathbf{j} + (v_z^{(1)} - a\omega_x^{(1)})\mathbf{k} = 0, \tag{7b}$$

$$(v_x^{(2)} + a\omega_z^{(2)})\mathbf{i} + (v_z^{(2)} - a\omega_x^{(2)})\mathbf{k} = 0. \tag{7c}$$

In words these conditions are, respectively: no tangential velocity at the end of the sliding period, no velocity at all at the end of the compression period, and no tangential velocity at the end of the recovery period.

B. Friction and restitution coefficient

Sliding is in the model of Crowe *et al.* modeled by Coulomb's law of friction. In order to know the tangential force—and therefore the tangential impulse— generated in the contact point during sliding, we require the normal force acting in the contact. While in evaluating the force acting on the particle as we did above, the two forces $F_{y,a}$ and $F_{y,t}$ were added, they must be subtracted to evaluate the normal force acting "in the contact point" (we keep in mind that the signs of $F_{y,a}$ and $F_{y,t}$ are always opposite so that the two forces physically act together in increasing the force acting in the contact point). The relation between the x, y, and z components of the force/impulse is

$$J_x^{(s)} = -\varepsilon_x f(J_{y,a}^{(s)} - J_{y,t}^{(s)}), \tag{8}$$

$$J_z^{(s)} = -\varepsilon_z f(J_{y,a}^{(s)} - J_{y,t}^{(s)}), \tag{9}$$

$$\varepsilon_x^2 + \varepsilon_z^2 = 1, \tag{10}$$

where f is Coulomb's coefficient of friction, and $(\varepsilon_x, \varepsilon_y)$ are the direction cosines for the sliding motion.

The standard definition of the coefficient of restitution for a particle colliding with a wall is as the ratio of the absolute value of the particle velocity, or momentum, normal to the plane of impact after the collision to that before the collision

$$e = \frac{v_y^{(2)}}{-v_y^{(0)}} = \frac{mv_y^{(2)}}{m(-v_y^{(0)})}. \tag{11}$$

In the model of Crowe *et al.*, this can also be written as the ratio of the impulse during the recovery period to that during the compression period

$$e = \frac{J_y^{(2)}}{J_y^{(1)}}. \tag{12}$$

Thus,

$$J_y^{(2)} = eJ_y^{(1)} = e(J_y^{(s)} + J_y^{(r)}). \tag{13}$$

If we, in the present model, wish to maintain a definition consistent with Eq. (11), we must define e as

$$e = \frac{J_{y,a}^{(2)} + J_{y,t}^{(2)}}{J_{y,a}^{(1)} + J_{y,t}^{(1)}}. \tag{14}$$

However, it is convenient for us to continue operating with the coefficient restitution due to the material deformation, i.e., the one defined by Eq. (12). Let us now call this e_m, defined by

$$e_m \equiv J_{y,a}^{(2)}/J_{y,a}^{(1)}. \tag{15}$$

This is also physically correct if we wish the coefficient of restitution to describe irreversibilities during the collision, leading to the loss of mechanical energy. With this, the equivalent of Eq. (13) is

$$J_y^{(2)} = J_{y,a}^{(2)} + J_{y,t}^{(2)} = e_m(J_{y,a}^{(s)} + J_{y,a}^{(r)}) + J_{y,t}^{(2)}, \tag{16}$$

the last equation being valid for case I only. Thus, e_m is here equivalent to the standard definition of e in Eq. (12), which is also given in Crowe [1].

1. Final equations for case I

We now solve the equations to obtain the final expressions for the translational and rotational velocity components of the particle leaving the collision. Combining equations Eqs. (5b) and (16) gives

$$m(v_y^{(2)} - v_y^{(1)}) = e_m(J_{y,a}^{(s)} + J_{y,a}^{(r)}) + J_{y,t}^{(2)}. \tag{17}$$

We note that $v_y^{(1)}$ is equal to zero [from the conditions on the surface velocity in the contact point; see Eqs. (7)]. Using this, and combining Eq. (17) with Eq. (3b) and Eq. (4b) leads to

$$v_y^{(2)} = e_m\left(-v_y^{(0)} - \frac{J_{y,t}^{(1)}}{m}\right) + \frac{J_{y,t}^{(2)}}{m}. \tag{18}$$

In the standard hard-sphere model we would derive here [1]

$$v_y^{(2)} = -ev_y^{(0)}. \tag{19}$$

Other components of particle velocity are derived exactly as in the standard hard-sphere model, since the new terms introduced in this paper are not present in the equations for x and z components,

$$v_x^{(2)} = \frac{5}{7}\left(v_x^{(0)} - \frac{2a}{5}\omega_z^{(0)}\right), \tag{20a}$$

$$v_z^{(2)} = \frac{5}{7}\left(v_z^{(0)} + \frac{2a}{5}\omega_x^{(0)}\right), \tag{20b}$$

$$\omega_x^{(2)} = v_z^{(2)}/a, \tag{20c}$$

$$\omega_y^{(2)} = \omega_y^{(0)}, \tag{20d}$$

$$\omega_z^{(2)} = -v_x^{(2)}/a. \tag{20e}$$

C. Case II

In this case the sliding period terminates in the recovery period.

The notation for the impulse components is as follows: we denote by superscript (1), (2), and (s) the impulses during the compression, the recovery and the part of the sliding period falling in the recovery period, respectively, and by superscript (r) the impulse during the "remainder" of the recovery period after the particle has stopped sliding.

The following model is proposed that is similar to the analogous equations describing case I,

$$m(v_x^{(1)} - v_x^{(0)}) = J_x^{(1)}, \tag{21a}$$

$$m(v_y^{(1)} - v_y^{(0)}) = J_{y,a}^{(1)} + J_{y,t}^{(1)}, \tag{21b}$$

$$m(v_z^{(1)} - v_z^{(0)}) = J_z^{(1)}, \tag{21c}$$

$$m(v_x^{(s)} - v_x^{(1)}) = J_x^{(s)}, \tag{22a}$$

$$m(v_y^{(s)} - v_y^{(1)}) = J_{y,a}^{(s)} + J_{y,t}^{(s)}, \tag{22b}$$

$$m(v_z^{(s)} - v_z^{(1)}) = J_z^{(s)}, \tag{22c}$$

$$m(v_x^{(2)} - v_x^{(s)}) = J_x^{(r)}, \tag{23a}$$

$$m(v_y^{(2)} - v_y^{(s)}) = J_{y,a}^{(r)} + J_{y,t}^{(r)}, \tag{23b}$$

$$m(v_z^{(2)} - v_z^{(s)}) = J_z^{(r)}, \tag{23c}$$

$$I(\omega_x^{(1)} - \omega_x^{(0)}) = -aJ_z^{(1)}, \tag{24a}$$

$$I(\omega_y^{(1)} - \omega_y^{(0)}) = 0, \tag{24b}$$

$$I(\omega_z^{(1)} - \omega_z^{(0)}) = aJ_x^{(1)}, \tag{24c}$$

$$I(\omega_x^{(s)} - \omega_x^{(1)}) = -aJ_z^{(s)}, \tag{24d}$$

$$I(\omega_y^{(s)} - \omega_y^{(1)}) = 0, \tag{24e}$$

$$I(\omega_z^{(s)} - \omega_z^{(1)}) = aJ_x^{(s)}, \tag{24f}$$

$$I(\omega_x^{(2)} - \omega_x^{(s)}) = -aJ_z^{(r)}, \tag{24g}$$

$$I(\omega_y^{(2)} - \omega_y^{(s)}) = 0, \tag{24h}$$

$$I(\omega_z^{(2)} - \omega_z^{(s)}) = aJ_x^{(r)}. \tag{24i}$$

The definition of the coefficient of restitution due to material deformation, e_m, is the same as before [Eq. (15)] leading to

$$J_{y,a}^{(2)} + J_{y,t}^{(2)} = J_{y,a}^{(s)} + J_{y,a}^{(r)} + J_{y,t}^{(2)} = e_m J_{y,a}^{(1)} + J_{y,t}^{(1)}. \tag{25}$$

Thus Eq. (21b) can be written as

$$m(v_y^{(1)} - v_y^{(0)}) = \frac{J_{y,a}^{(2)}}{e_m} + J_{y,t}^{(1)}, \tag{26}$$

which is the same as

$$m(v_y^{(1)} - v_y^{(0)}) = \frac{J_{y,a}^{(s)} + J_{y,a}^{(r)}}{e_m} + J_{y,t}^{(1)}. \tag{27}$$

We further impose the conditions that the tangential component of surface velocity of the particle in the contact point is zero at the end of the sliding and recovery periods similarly to Eqs. (7a) and (7c) and that the y component of the translational velocity is zero at the end of the compression period, $v_y^{(1)} = 0$. We again use Coulombs law of friction to relate the normal stresses to the tangential ones, in this case both during the compression period and the part of the sliding period falling in the recovery period, similarly to Eqs. (8)–(10).

Taking into account the condition $v_y^{(1)} = 0$, as well as Eqs. (22b) and (23b), we derive

$$v_y^{(2)} = e_m\left(-v_y^{(0)} - \frac{J_{y,t}^{(1)}}{m}\right) + \frac{J_{y,t}^{(2)}}{m}, \tag{28}$$

which is the same as Eq. (18).

The remaining results, i.e., for the x and z components of the linear velocity, as well as all the components of the angular velocity are the same as in the standard hard-sphere model and the same as in case I.

D. Case III

The third case is the situation where the particle continues to slide also throughout the recovery period. We denote by superscript (1) and (2) the impulses during the compression and the recovery periods, respectively.

For this case the following model is proposed:

$$m(v_x^{(1)} - v_x^{(0)}) = J_x^{(1)}, \tag{29a}$$

$$m(v_y^{(1)} - v_y^{(0)}) = J_{y,a}^{(1)} + J_{y,t}^{(1)}, \tag{29b}$$

$$m(v_z^{(1)} - v_z^{(0)}) = J_z^{(1)}, \tag{29c}$$

$$m(v_x^{(2)} - v_x^{(1)}) = J_x^{(2)}, \tag{30a}$$

$$m(v_y^{(2)} - v_y^{(1)}) = J_{y,a}^{(2)} + J_{y,t}^{(2)}, \tag{30b}$$

$$m(v_z^{(2)} - v_z^{(1)}) = J_z^{(2)}, \tag{30c}$$

$$I(\omega_x^{(1)} - \omega_x^{(0)}) = -aJ_z^{(1)}, \tag{31a}$$

$$I(\omega_y^{(1)} - \omega_y^{(0)}) = 0, \tag{31b}$$

$$I(\omega_z^{(1)} - \omega_z^{(0)}) = aJ_x^{(1)}, \tag{31c}$$

$$I(\omega_x^{(2)} - \omega_x^{(1)}) = -aJ_z^{(2)}, \tag{31d}$$

$$I(\omega_y^{(2)} - \omega_y^{(1)}) = 0, \tag{31e}$$

$$I(\omega_z^{(2)} - \omega_z^{(1)}) = aJ_x^{(2)}. \tag{31f}$$

Also for this case we have

$$v_y^{(1)} = 0. \tag{32}$$

We define the restitution coefficient due to material deformation in the same way as in the previous section [see Eq. (15)]. Equation (30b) can thus be written as

$$m(v_y^{(2)} - v_y^{(1)}) = e_m J_{y,a}^{(1)} + J_{y,t}^{(2)}. \tag{33}$$

Using Eq. (29b) and after some arrangement, the final equation for $v_y^{(2)}$ becomes the same as for cases I and II,

$$v_y^{(2)} = e_m\left(-v_y^{(0)} - \frac{J_{y,t}^{(1)}}{m}\right) + \frac{J_{y,t}^{(2)}}{m}. \tag{34}$$

Also for this case we use Coulomb's law of friction,

$$J_x^{(1)} = -\varepsilon_x f(J_{y,a}^{(1)} - J_{y,t}^{(1)}), \tag{35a}$$

$$J_z^{(1)} = -\varepsilon_z f(J_{y,a}^{(1)} - J_{y,t}^{(1)}), \tag{35b}$$

$$J_x^{(2)} = -\varepsilon_x f(J_{y,a}^{(2)} - J_{y,t}^{(2)}), \tag{35c}$$

$$J_z^{(2)} = -\varepsilon_z f(J_{y,a}^{(2)} - J_{y,t}^{(2)}). \tag{35d}$$

Use of Eqs. (29a), (29b), (32), and (35a) leads to the following equation:

$$v_x^{(1)} = v_x^{(0)} + \varepsilon_x f\left(v_y^{(0)} + 2\frac{J_{y,t}^{(1)}}{m}\right). \tag{36}$$

Further use of Eqs. (30a), (30b), (32), and (35c), as well as (36) results in the following equation for $v_x^{(2)}$:

$$v_x^{(2)} = v_x^{(0)} + \varepsilon_x f v_y^{(0)}(1 + e_m) + \varepsilon_x f\left[(2 + e_m)\frac{J_{y,t}^{(1)}}{m} + \frac{J_{y,t}^{(2)}}{m}\right]. \tag{37}$$

The same procedure may be used for deriving the final expression for the z component of the postcollisional translational velocity, $v_z^{(2)}$,

$$v_z^{(2)} = v_z^{(0)} + \varepsilon_z f v_y^{(0)}(1 + e_m) + \varepsilon_z f\left[(2 + e_m)\frac{J_{y,t}^{(1)}}{m} + \frac{J_{y,t}^{(2)}}{m}\right]. \tag{38}$$

We proceed to find the components of the angular velocity after the collision. We start by using Eqs. (29b), (31a), and (35b) to find the following expression for the angular velocity after the compression period:

$$\omega_x^{(1)} = \omega_x^{(0)} - \frac{5}{2a}\varepsilon_z f\left(v_y^{(0)} + 2\frac{J_{y,t}^{(1)}}{m}\right). \tag{39}$$

The final result for $\omega_x^{(2)}$ is obtained from this equation together with Eqs. (31d), (35d), (30b), and (32),

$$\omega_x^{(2)} = \omega_x^{(0)} - \frac{5}{2a}\varepsilon_z f v_y^{(0)}(e_m + 1) - \frac{5}{2a}\varepsilon_z f\left[(2 + e_m)\frac{J_{y,t}^{(1)}}{m} + \frac{J_{y,t}^{(2)}}{m}\right]. \tag{40}$$

In a similar way we obtain the final result for $\omega_z^{(2)}$,

$$\omega_z^{(2)} = \omega_z^{(0)} + \frac{5}{2a}\varepsilon_x f v_y^{(0)}(e_m + 1) + \frac{5}{2a}\varepsilon_x f\left[(2 + e_m)\frac{J_{y,t}^{(1)}}{m} + \frac{J_{y,t}^{(2)}}{m}\right]. \tag{41}$$

The final result for $\omega_y^{(2)}$ is the same as in the other two cases,

$$\omega_y^{(2)} = \omega_y^{(0)}. \tag{42}$$

We note that this case is, both here and in the original hard-sphere model, not fully solved, since the direction cosines during the sliding collision, ε_x and ε_z, appear in the solutions for the final velocity components. These direction cosines are in principle unknown, since the particle—depending on the direction of rotation—can veer off from its translational path during the collision.

E. Conditions for occurrence of the cases

We have now derived the expressions for the translational and rotational movement of the particle emerging from the collision for each of the three cases. The only question that remains is how to distinguish between the cases so that we know which set of solutions to use for a specific situation.

As shown case I and case II, although different in principle, lead to the same results. Therefore it is enough to distinguish between cases II and III.

Matsumoto and Saito [31] show how to distinguish between the two cases for the standard hard-sphere model. Their description is based on a two-dimensional (2D) collision. In the following, we give a detailed description of a model that makes it possible to distinguish between the cases for a three-dimensional (3D) collision with adhesion forces, i.e., for the mathematical model developed in this paper. We are basing this discussion on the paper of Matsumoto and Saito.

The strategy is to derive expressions for the total normal and tangential impulses during the collision, and compare the tangential one with the one expected from Coulombs law of friction. If the tangential impulse is lower than that expected

from Coulombs law, sliding will have stopped sometimes during the collision.

We begin by writing the system of impulse equations that is valid for any point in time during the collision:

$$m(v_x - v_x^{(0)}) = J_x, \tag{43a}$$

$$m(v_y - v_y^{(0)}) = J_y, \tag{43b}$$

$$m(v_z - v_z^{(0)}) = J_z, \tag{43c}$$

and for the rotation,

$$I(\omega_x - \omega_x^{(0)}) = -aJ_z, \tag{44a}$$

$$I(\omega_y - \omega_y^{(0)}) = 0, \tag{44b}$$

$$I(\omega_z - \omega_z^{(0)}) = aJ_x. \tag{44c}$$

The velocity of the particle surface at the contact point (denoted by sub-r) is

$$v_{x,r} = v_x + a\omega_z, \tag{45a}$$

$$v_{y,r} = v_y, \tag{45b}$$

$$v_{z,r} = v_z - a\omega_x, \tag{45c}$$

which for the initial state becomes

$$v_{x,r}^{(0)} = v_x^{(0)} + a\omega_z^{(0)}, \tag{46a}$$

$$v_{y,r}^{(0)} = v_y^{(0)}, \tag{46b}$$

$$v_{z,r}^{(0)} = v_z^{(0)} - a\omega_x^{(0)}. \tag{46c}$$

With the help of the above equations and using the fact that for a sphere of radius a the moment of inertia $I = (2/5)a^2 m$, we can write the particle surface velocity in the contact point during the collision in terms of its initial value (its value just before the collision).

$$v_{x,r} = v_{x,r}^{(0)} + \frac{7}{2}\frac{J_x}{m}, \tag{47a}$$

$$v_{y,r} = v_{y,r}^{(0)} + \frac{J_y}{m}, \tag{47b}$$

$$v_{z,r} = v_{z,r}^{(0)} + \frac{7}{2}\frac{J_z}{m}. \tag{47c}$$

At the end of the compression period $v_{y,r}=0$, so find the normal impulse acting on the particle during the compression period, $J_y^{(1)}$, we insert this in Eq. (47b) to obtain

$$J_y^{(1)} = -mv_{y,r}^{(0)}. \tag{48}$$

This impulsive force comprises both the interaction due to material deformation and that due to the adhesive forces, i.e., $J_y^{(1)} = J_{y,a}^{(1)} + J_{y,t}^{(1)}$.

The y component of the impulse acting during the recovery period is $J_y^{(2)} = J_{y,a}^{(2)} + J_{y,t}^{(2)}$. Using Eq. (15), we can also

write: $J_y^{(2)} = e_m J_{y,a}^{(1)} + J_{y,t}^{(2)}$. Thus an expression for the total normal impulse during the whole collision is

$$J_{y,tot} = J_y^{(1)} + J_y^{(2)} = -mv_{y,r}^{(0)} + e_m J_{y,a}^{(1)} + J_{y,t}^{(2)} \tag{49}$$

and since $J_{y,a}^{(1)} = J_y^{(1)} + J_{y,t}^{(1)}$,

$$J_{y,tot} = -mv_{y,r}^{(0)}(1 + e_m) + e_m J_{y,t}^{(1)} + J_{y,t}^{(2)}. \tag{50}$$

We now derive an expression for the tangential impulse acting on the particle in the contact point: $J_t = \sqrt{J_x^2 + J_z^2}$, which equals the tangential impulse at the end of the sliding period.

Using Eqs. (47) and taking into account that at the end of the sliding period $v_{x,r} = v_{z,r} = 0$ we obtain for the tangential impulse during the entire collision,

$$J_{t,tot} = \frac{2}{7}m\sqrt{(v_{x,r}^{(0)})^2 + (v_{z,r}^{(0)})^2}. \tag{51}$$

Case I or II occur, as mentioned, if this is lower than the value expected from Coulombs law of friction $J_{t,tot} \leq J_{y,tot} f$ giving the criterion

$$\frac{2}{7}m\sqrt{(v_x^{(0)} + a\omega_z^{(0)})^2 + (v_z^{(0)} - a\omega_x^{(0)})^2}$$

$$\leq [-mv_y^{(0)}(1 + e_m) + e_m J_{y,t}^{(1)} + J_{y,t}^{(2)}]f. \tag{52}$$

For zero adhesive force this criterion reduces to that in Crowe *et al.* [1] and in 2D to that in Matsumoto and Saito [31] (who, however, had the y axis reversed compared to this study).

F. Condition for deposition

Our model including adhesion distinguishes between the two cases:

(i) "deposition" and

(ii) "rebound,"

and we now derive a criterion for which case applies.

We know already that the total impulse in the y direction is described by Eq. (50). Since $v_{y,r}^{(0)} = v_y^{(0)}$ we can also write

$$J_{y,tot} = -mv_y^{(0)}(1 + e_m) + e_m J_{y,t}^{(1)} + J_{y,t}^{(2)}. \tag{53}$$

The particle will rebound after the collision if its velocity in the y direction, $v_y^{(2)}$, is greater than zero. We conclude from the fundamental relation: $m(v_y^{(2)} - v_y^{(0)}) = J_{y,tot}$ that $v_y^{(2)} > 0$ if $J_{y,tot} > -mv_y^{(0)}$ and substituting for $J_{y,tot}$ from Eq. (53), we arrive at the condition for the rebounding to take place,

$$v_y^{(0)} < \frac{1}{e_m m}(J_{y,t}^{(2)} - e_m J_{y,t}^{(1)}). \tag{54}$$

If this condition is not satisfied, the y component of particle velocity after the collision will be negative (deposition). In practice, it can be set to zero.

Note that in the standard hard-sphere model the impulses $J_{y,t}^{(1)}$ and $J_{y,t}^{(2)}$ are zero. Thus, if $e_m > 0$, the above condition becomes

$$v_y^{(0)} < 0, \tag{55}$$

which is always true since the y component of the initial velocity is always negative. Thus the deposition will never

occur in the standard hard-sphere model if $e_m > 0$.

The above condition can also be derived in a more heuristic way. As the particle approaches the wall, it will encounter the attractive force, and in response to the impulse, $J_{y,t}^{(1)}$, it will attain a y velocity "higher" (more negative) by $\Delta v_y^{(1)}$, say, than the one it would have had in the absence of $J_{y,t}^{(1)}$. Conversely, on the way out after rebounding, it will be decelerated by $\Delta v_y^{(2)}$ (which is also negative) due to the attractive (and thus negative) impulse $J_{y,t}^{(2)}$. The y velocity out will thus be

$$v_y^{(2)} = -e_m(v_y^{(0)} + \Delta v_y^{(1)}) + \Delta v_y^{(2)}. \tag{56}$$

Remembering that $\Delta v_y^{(\cdot)} = J_{y,t}^{(\cdot)}/m$ leads to the same criterion as Eq. (54) for $v_y^{(2)}$ to be greater than zero.

G. Model for $J_{y,t}$

To close the system of equations we need to find expressions for the impulses acting during the compression and recovery periods: $J_{y,t}^{(1)}$ and $J_{y,t}^{(2)}$, since these terms represent new variables in addition to those present in the original hard-sphere model. They can be written in the integral form,

$$J_{y,t}^{(1)} = \int_0^{t_1} F_{y,t} dt \tag{57}$$

and

$$J_{y,t}^{(2)} = \int_{t_1}^{t_2} F_{y,t} dt, \tag{58}$$

where $F_{y,t}$ is the force acting on the particle in the downward direction, t_1 is the time of compression period, t_2 is the total collision time so that $t_2 - t_1$ is the time of the recovery period.

The attractive force acting during a collision may be due to, for example, van der Waals forces or liquid bridging. In both cases the force will act not only during contact but also over short distances during approach and possible departure. To find the impulses we therefore need to include short periods before and after the collision in the "compression" and "recovery" periods, respectively.

The potential of the force will constitute a potential well, and irreversibilities during the collision will give rise to the loss of mechanical energy, possibly resulting in the particle not being able to escape this potential well on its way out.

Such irreversibilities are described by the coefficient of restitution, and may physically be due to:

(i) plastic deformation of the particle and/or the wall material;

(ii) irreversibilities in the adhesion process resulting from the reorganization of molecules during the contact period [25].

(iii) viscous dissipation in the fluid between the particle and the wall squeezed out during approach and sucked in during departure. This can be dissipation in the carrier fluid in which the collision takes place [1] or in the fluid contained in a liquid bridge formed between the particle and the wall.

Quantification of either the coefficient of restitution, e_m or the impulse due to attraction $J_{y,t}$ from the physics is not the focus of this paper. Theories for Hamaker interaction and

interaction during contact, such as the JKR theory, or for interaction through liquid bridging may assist in formulating semiempirical quantifications of $J_{y,t}$ [34]. Normally we know the attractive force as a function of surface separation, D say, not time, and to obtain the integral over time for the impulse we need to change variables, e.g., for the (extended) compression period

$$\int_0^{t_1} F_{y,t}(t) dt = \int_{D_1}^{D_c} F_{y,t}(D) \frac{dt}{dD} dD = \int_{D_1}^{D_c} \frac{F_{y,t}(D)}{v_y(D)} dD, \tag{59}$$

where D_1 is the surface separation at some point in time before the collision where the interaction force is still negligible, and D_c is the surface separation at the end of the compression period. The need to carry out this change of variables makes quantification of the impulses difficult even for very simple functional forms for $F_{y,t}(D)$, since we require $v_y(D)$, which itself is a function of $F_{y,t}(D)$ as well as a function of the properties of the particle and the wall. Even in case of the simple functional form of Hamaker interaction between a spherical body and a flat plate [25] acting during the approach and possible departure,

$$F_{y,t}(D) = -\frac{A}{6D^2} a, \tag{60}$$

where A is the Hamaker constant and a the radius of the spherical body there is no analytical solution that we are aware of to the problem of changing the variable of integration from D to t in Eq. (59).

We note that Weber *et al.* [27], when faced with the same difficulties in their implementation of particle cohesion in a numerical scheme, used a simple "square-well" potential, which implies that a Dirac delta-type force acts between particles at a particular separation.

We choose in this case a similar simple interaction model, but prefer to use a constant force acting over a certain range of surface separations, namely, between a surface separation where the Hamaker interaction can be considered negligible to the surface separation at "contact." We thus neglect attractive impulse during the period of actual contact between the particle and the wall.

If the force $F_{y,t}$ can be taken as constant during the collision then the integrals for the impulse become

$$J_{y,t}^{(1)} = F_{y,t} t_1 \tag{61}$$

and

$$J_{y,t}^{(2)} = F_{y,t}(t_2 - t_1). \tag{62}$$

So that it only remains to quantify $F_{y,t}$ and find the times during which it acts, i.e., finding t_1 and t_2. This, however, is not a simple task either. The value of $F_{y,t}$ reflecting correctly, say, Hamaker interaction will depend on the velocity profile of the particle when it is within the range of the attractive force, and also t_1 and t_2 will depend not only on the initial and final translational velocities, but also on the magnitude of the attractive force itself and the inertia of the particle.

So, for this paper we choose this constant force to be only in some measure equivalent to the force acting due to Hamaker interactions by using the spatially mean value of Hamaker force over the separations where the Hamaker force is significant.

We can with Weber *et al.* [27] assume the Hamaker force to be negligible when it equals the force of gravity acting on the particle. This happens at a surface separation of D_1 for which

$$-\frac{A}{6D_1^2}a = \frac{4}{3}\pi a^3 \rho g_z \Rightarrow D_1 = \sqrt{\frac{A}{8a^2\rho g_z \pi}}. \qquad (63)$$

D_1 comes to about 10 nm if the particle has a density of 1000 kg/m^3, a radius of 20 μm and the Hamaker constant is $A=10^{-20}$ J.

We assume that the surface separation at "contact," D_c say, is 2 nm [25]. The mean force, which should be applied at surface separations in the range D_1-D_c is

$$F_{y,t} = \frac{\int_{D_c}^{D_1} -\frac{A}{6D^2}adD}{(D_1-D_c)} = \frac{Aa}{6(D_1-D_c)}\left(\frac{1}{D_1}-\frac{1}{D_c}\right) = -\frac{Aa}{6D_cD_1}. \qquad (64)$$

To find $v(D)$ for use in Eq. (59), we write down Newton's second law, resolved in the y direction, for a particle on which this force is acting,

$$m\frac{dv_y}{dt} = m\frac{dv_y}{dD}\frac{dD}{dt} = m\frac{dv_y}{dD}v_y = F_{y,t}, \qquad (65)$$

where m is the particle mass. This equation is variables separable, and can be integrated directly. We now consider the particle's approach to the collision and its (possible) departure from the collision separately:

Approach. Here we integrate Eq. (65) between the limits D_1, where the y velocity is $v_y^{(0)}$ and an arbitrary surface separation D, where the velocity is v_y, giving

$$v_y(D) = -\sqrt{\frac{2F_{y,t}}{m}(D-D_1) + (v_y^{(0)})^2}. \qquad (66)$$

Inserting this expression for $v(D)$ in Eq. (59) and carrying out the integration results in

$$J_{y,t}^{approach} = J_{y,t}^{(1)} = -m\left(\sqrt{\frac{2F_{y,t}(D_c-D_1)}{m} + (v_y^{(0)})^2} - |v_y^{(0)}|\right). \qquad (67)$$

The velocity of the particle at impact, say v_1, can be found by inserting $D=D_c$ in Eq. (66),

$$v_1 = v_y(D_c) = -\sqrt{\frac{2F_{y,t}}{m}(D_c-D_1) + (v_y^{(0)})^2}. \qquad (68)$$

Please note that v_y is negative before impact.

Departure. Here we integrate Eq. (65) between the limits $D=D_c$, where the y-velocity is $v_2=-v_1e_m$ and an arbitrary surface separation, D, where the velocity is v_y,

$$v_y(D) = \sqrt{\frac{2F_{y,t}}{m}(D-D_c) + v_2^2}. \qquad (69)$$

Inserting this expression for $v(D)$ in Eq. (59) and carrying out the integration results in

$$J_{y,t}^{departure} = J_{y,t}^{(2)} = m\left(\sqrt{\frac{2F_{y,t}(D_1-D_c)}{m} + v_2^2} - v_2\right). \qquad (70)$$

Please note that the argument under the root sign can be negative if the initial starting velocity v_2 is too low or/and the force $F_{y,t}$ is too high. This corresponds to the case when the particle deposits on the surface, i.e., it is not able to leave the zone where the van der Waals force acts. Thus deposition will take place if

$$\frac{2F_{y,t}(D_1-D_c)}{m} + v_2^2 \leq 0 \qquad (71)$$

and taking into account Eq. (68) and the relation $v_2=-v_1e_m$, we obtain

$$-\frac{2F_{y,t}(D_1-D_c)}{m}\left(\frac{1}{e_m^2}-1\right) \geq (v_y^{(0)})^2. \qquad (72)$$

Because $F_{y,t}$ is negative, the left-hand side of the inequality is positive. Thus we can easily estimate the minimum value of the initial velocity v_0 that leads to deposition on the surface. We can now come back to our extension of the hard-sphere model and insert the new impulsive forces defined by Eqs. (67) and (70).

III. SIMULATION RESULTS

In this section we show some examples where our extended hard-sphere model is compared with the standard one and the effect of the attractive force is illustrated. First we investigate the simple case where one particle with a diameter of 1 μm collides with a wall. Two components of the initial velocity are fixed: $v_x^{(0)}=1.0$ and $v_z^{(0)}=0.0$, while $v_y^{(0)}$ will vary for different cases. The restitution coefficient, e_m, is equal to 0.9, while the Coulombian friction factor, f, is taken as 0.15 (these values are typical for many applications in applications involving granular materials). The Hamaker constant is equal to 10×10^{-20} J and the particle diameter is 1000 kg/m^3.

The calculation results for this example are shown in Fig. 3. What we present is the y component of the velocity after the collision, $v_y^{(2)}$, as a function of the initial y component, $v_y^{(0)}$. The figure thus represents a range of collisions with varying approach velocities. The two curves on the graph compare the standard hard-sphere model with our extended model.

The main difference is at the lower initial velocities. The standard hard-sphere model is not able to simulate deposition and the particles bounce off even under conditions where deposition might be expected. Also for the cases when no deposition occurs, the emerging velocity is too high.

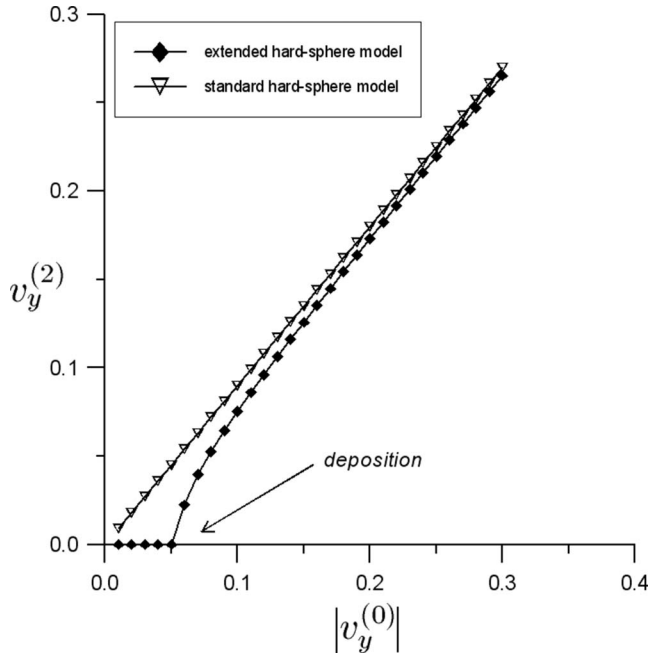We emphasize here, however, that for many practical applications where the effect of adhesion is negligible (e.g.,

FIG. 3. The y component of particle velocity after impact, $v_y^{(2)}$ computed for various values of the initial value of this component $v_y^{(0)}$. The particle diameter is 1 μm and the restitution and friction coefficients are 0.9 and 0.15, respectively. The model for adhesion force is as described in Sec. II F.

flows with high velocities and big particles), the standard hard-sphere model is sufficient.

Since the particle diameter is an important parameter in determining when deposition take place, we investigate its influence on the results by calculating the limiting approach velocity, $v_y^{(0)}$, at which deposition will take place, we can call this limiting velocity v_0. To do this we insert Eq. (60) into Eq. (72) so that we obtain a function $v_0 = f(a)$, where a is the radius of the particle

$$|v_y^{(0)}| = \frac{2}{a}\left[\frac{A(D_1 - D_c)}{4\pi D_c D_1 \rho}\left(\frac{1}{e_m^2} - 1\right)\right]^{1/2}, \qquad (73)$$

where we have used the relation for the particle mass $m = \rho \frac{4\pi a^3}{3}$.

The function is shown in Fig. 4 where all other parameters (restitution coefficient, Hamaker constant etc.) are the same as above. We have also marked the two domains that correspond to the case where the particle deposits on the surface and bounces off, respectively.

The model shown in this paper, as well as the results presented in this section, refers to a single particle only. The collision model may be implemented in Eulerian-Lagrangian numerical simulations based on the tracking of individual particles, where, between collisions, forces acting on the particles such as fluid-particle interactions must be considered. Thus our model can be used for any system of particles, just like the standard hard-sphere model.
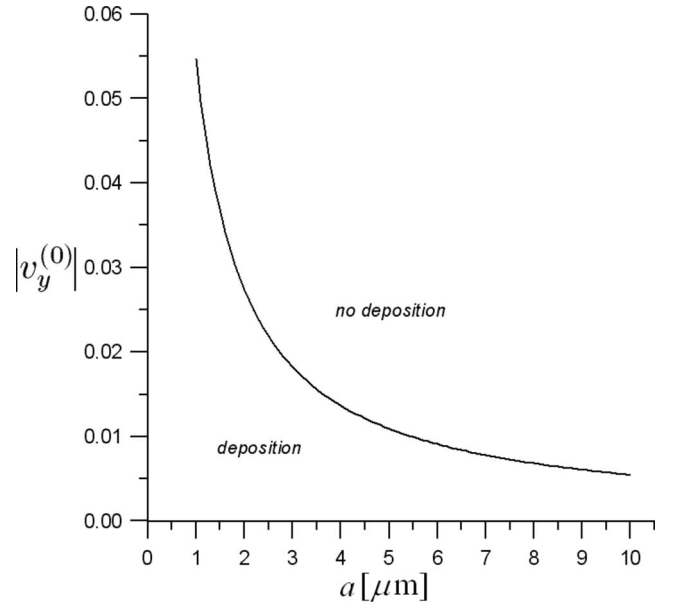

FIG. 4. The graphical interpretation of Eq. (73).

IV. CONCLUDING REMARKS

In this paper we developed an extension of the standard hard-sphere particle-wall collision model to account for particle adhesion. This extension of the model makes it possible to account for any interaction acting in addition to the "usual" mechanical collision as long as we know its mathematical formulation. This was done by modifying the hard-sphere model described in detail in Crowe *et al.* [1].

As an example we implemented a van-der-Waals-like interaction, where we assumed a constant force to act equal to the average of the van der Waals force over the range of interaction. This to illustrate the effect of the extension to the model in practical applications.

In the near future we wish to continue this research in more than one direction. It is of interest, to quantify the adhesion interaction building on the literature on this topic, e.g., to describe the van der Waals interaction using more correct approximations and simplify this in a physically realistic way, such that it can be implemented in the collision model. We will also formulate equations for particle-particle collisions to model cohesion and the formation of aggregates.

[1] C. Crowe, M. Sommerfeld, and Y. Tsuji, *Multiphase Flow with Droplets and Particles* (CRC Press, New York, 1998).

[2] A. Castellanos, J. M. Valverde, and M. A. S. Quintanilla, Phys. Rev. E **64**, 041304 (2001).

[3] H. Lu, Z. Shen, J. Ding, L. Xiang, and H. Liu, Powder Technol. **169**, 159 (2006).

[4] H. Lu, Y. Zhao, J. Ding, D. Gidaspow, and L. Wei, Chem. Eng. Sci. **62**, 301 (2007).

[5] E. Helland, R. Occelli, and L. Tadrist, Chem. Eng. Sci. **60**, 27 (2005).

[6] N. G. Deen, M. Van Sint Annaland, M. A. Van der Hoef, and J. A. M. Kuipers, Chem. Eng. Sci. **62**, 28 (2007).

[7] N. Mitarai and H. Nakanishi, Phys. Rev. E **67**, 021301 (2003).

[8] J. Ouyang and A. B. Yu, Part. Sci. Technol. **23**, 47 (2005).

[9] X. Y. Zhang and G. Ahmadi, Chem. Eng. Sci. **60**, 5089 (2005).

[10] M. van Sint Annaland, N. G. Deen, and J. A. M. Kuipers, Chem. Eng. Sci. **60**, 6188 (2005).

[11] C. L. Wu, J. M. Zhan, Y. S. Li, and K. S. Lam, Chem. Eng. Sci. **61**, 5726 (2006).

[12] R. Brewster, L. E. Silbert, G. S. Grest, and A. J. Levine, Phys. Rev. E **77**, 061302 (2008).

[13] R. Brewster, G. S. Grest, and A. J. Levine, Phys. Rev. E **79**, 011305 (2009).

[14] P. Kosinski, Shock Waves **15**, 13 (2006).

[15] P. Kosinski and A. C. Hoffmann, Comput. Fluids **36**, 714 (2007).

[16] C. G. Ilea, P. Kosinski, and A. C. Hoffmann, Chem. Eng. Sci. **63**, 3864 (2008).

[17] B. P. B. Hoomans, J. A. M. Kuipers, W. J. Briels, and W. P. M. van Swaaij, Chem. Eng. Sci. **51**, 99 (1996).

[18] J. Visser, Powder Technol. **58**, 1 (1989).

[19] J. P. K. Seville, C. D. Willett, and P. C. Knight, Powder Technol. **113**, 261 (2000).

[20] T. Mikami, H. Kamiya, and M. Horio, Chem. Eng. Sci. **53**, 1927 (1998).

[21] Y. Tsuji, T. Kawaguchi, and T. Tanaka, Powder Technol. **77**, 79 (1993).

[22] G. Lian, C. Thornton, and M. J. Adams, Chem. Eng. Sci. **53**, 3381 (1998).

[23] G. Lian, M. J. Adams, and C. Thornton, J. Fluid Mech. **311**, 141 (1996).

[24] J. Baxter, H. Abou-Chakra, U. Tuzun, and B. M. Lamptey, Chem. Eng. Res. Des. **78**, 1019 (2000).

[25] J. N. Israelachvili, *Intermolecular and Surface Forces, Second Edition: With Applications to Colloidal and Biological Systems*, 2nd ed. (Academic Press, New York, 1992).

[26] J. K. Pandit, X. S. Wang, and M. J. Rhodes, Powder Technol. **160**, 7 (2005).

[27] M. W. Weber, D. K. Hoffman, and C. M. Hrenya, Granular Matter **6**, 239 (2004).

[28] M. W. Weber and C. M. Hrenya, Chem. Eng. Sci. **61**, 4511 (2006).

[29] K. L. Johnson, K. Kendall, and A. D. Roberts, Proc. R. Soc. London, Ser. A **324**, 301 (1971).

[30] B. V. Derjaguin, V. M. Muller, and Yu. P. Toporov, J. Colloid Interface Sci. **53**, 314 (1975).

[31] S. Matsumoto and S. Saito, J. Chem. Eng. Jpn **3**, 223 (1970).

[32] M. Sommerfeld and N. Huber, Int. J. Multiphase Flow **25**, 1457 (1999).

[33] Y. Tsuji, Y. Morikawa, T. Tanaka, N. Nakatsukasa, and M. Nakatani, Int. J. Multiphase Flow **13**, 671 (1987).

[34] N. V. Brilliantov, N. Albers, F. Spahn, and T. Poschel, Phys. Rev. E **76**, 051302 (2007).